LBL-21856

Lawrence Berkeley Laboratory
UNIVERSITY OF CALIFORNIA

Materials & Molecular
Research Division

Invited paper presented at the Symposium on
Relativistic Many-Body Problems, Trieste, Italy,
June 30-July 4, 1986; and to be published in
Physica Scripta

TESTS OF QUANTUM ELECTRODYNAMICS IN FEW-ELECTRON VERY HIGH-Z IONS

H. Gould and C.T. Munger

August 1986

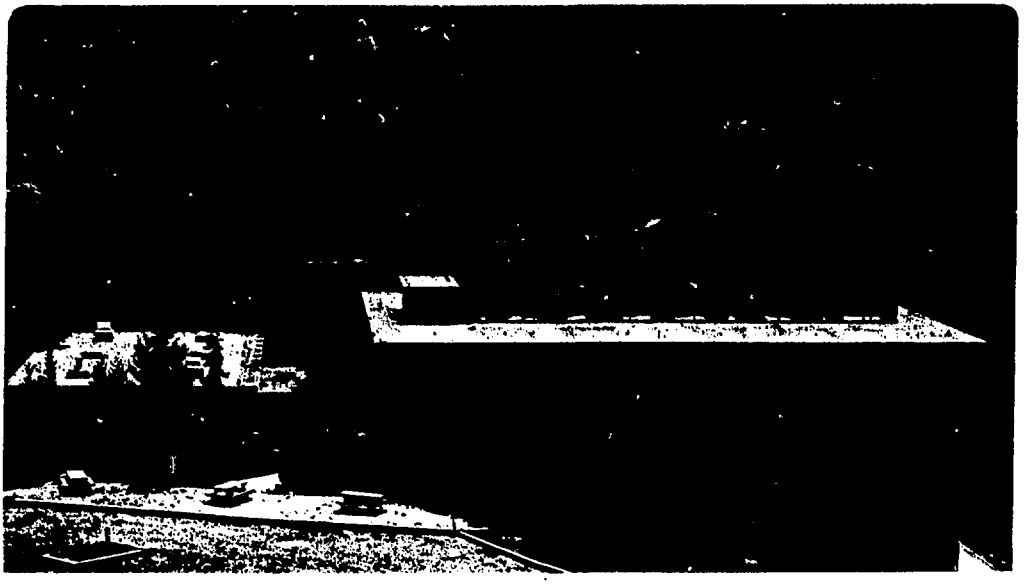

Prepared for the U.S. Department of Energy under Contract DE-AC03-76SF00098

TESTS OF QUANTUM ELECTRODYNAMICS IN FEW-ELECTRON VERY HIGH-Z IONS

Harvey Gould and Charles T. Munger

Materials and Molecular Research Division,
building 71-259, Lawrence Berkeley Laboratory,
University of California, Berkeley, California 94720

LBL--21856

DE87 000124

Abstract

This article discusses our measurement of the Lamb shift in heliumlike uranium and outlines future tests of QED using few- electron very high atomic number (Z) ions. Our recently reported Lamb shift value of 70.4 (8.1) eV for the one- electron Lamb shift in uranium is in agreement with the theoretical value of 75.3 (0.4) eV. The experimental value was extracted from a beam-foil time-of-flight measurement of the 54.4 (3.3) ps lifetime of the $1s2p_{1/2}\ ^3P_0$ state of heliumlike uranium.

1. Lamb Shift in Heliumlike Uranium

1.1 Self-energy in very high Z atoms.

A possible failure of quantum electrodynamics (QED) to predict accurate radiative corrections to bound states at Z= 92 is not ruled out by its success at low Z. The largest contribution to the Lamb shift at Z = 92 comes from terms in the electron self-energy[1] which are high powers of $Z\alpha$ and which are invisible in experiments at low Z. Lamb shift measurements on high-Z electronic and muonic atoms are complementary because muonic atom measurements are sensitive to higher order vacuum polarization effects but not to self-energy effects[2].

The contribution of the higher order terms in the self-energy can be seen

by comparing the series expansion of the self energy with an evaluation of the self-energy to all orders in $Z\alpha$. If we write the self energy Σ_n in a power series in α and $Z\alpha$, we have:

$$\Sigma_n = n^{-3}(\alpha/\pi)\, m_o c^2 \Big[[A_{40} + A_{41}\ln(Z\alpha)^{-2}](Z\alpha)^4 + A_{50}(Z\alpha)^5 + [A_{60} + A_{61}\ln(Z\alpha)^{-2} + A_{62}\ln^2(Z\alpha)^{-2}](Z\alpha)^6 + A_{70}(Z\alpha)^7 + \text{higher order terms} \Big] \quad (1)$$

Where n is the principal quantum number and m_o is the electron rest mass. Values of the coefficients $A_{40} - A_{70}$ can be found in Ref. 1. Fig. 1 shows the ratio of the higher order terms in the self-energy to the total self energy. In neutral hydrogen the higher order terms in the self-energy are negligible but at Z=92 they are the largest contribution to the Lamb shift.

1.2 Lamb shift from the lifetime of the $1s2p_{1/2}\ ^3P_0$ state of heliumlike uranium

We choose heliumlike uranium over hydrogenlike uranium for this measurement because the n=2 states of hydrogenlike uranium decay very rapidly making it difficult to observe the decays outside of the target where the hydrogenlike uranium is formed. If the decay inside the target is observed there is the risk that the measurement will be in error because the target perturbs the energy levels of the atom. In heliumlike uranium, however, the $1s2p_{1/2}\ ^3P_0$ state (Fig. 2) is metastable and it's decay in vacuum can be observed downstream from the target.

In heliumlike uranium the $1s2p_{1/2}\ ^3P_0$ state decays 70% of the time to the $1s2s\ ^3S_1$ state by an electric-dipole (E1) transition. This makes the $1s2p_{1/2}\ ^3P_0$ lifetime sensitive to the $1s2p_{1/2}\ ^3P_0$ - $1s2s\ ^3S_1$ energy difference of 260.0 (7.8) eV and hence to the Lamb shift. At Z=92 the major contributions to the calculated Lamb shift are the self-energy[3] of 56.7 eV, the leading order term in the vacuum polarization[3,4] of -14.3 eV and the finite nuclear size correction[4] of 32.5 eV. In heliumlike uranium there is also a small screening correction to the radiative corrections - expected to be of order 1/Z times the self-energy[2,5]. For zero Lamb shift the $1s2p_{1/2}\ ^3P_0$ - $1s2s\ ^3S_1$ states would be split by the difference in the $1s_{1/2}$ - $2s_{1/2}$ and $1s_{1/2}$ - $2p_{1/2}$ Coulomb interactions. This splitting at Z = 92 has been calculated by Mohr[6] to be 330.4 eV, which agrees (1 eV) with the calculations of Lin, Johnson and Dalgarno[7] and of Drake[8]. The other significant decay of the $1s2p_{1/2}\ ^3P_0$ state is to the $1s^2\ ^1S_0$ ground state by a two-photon electric-dipole

magnetic-dipole (E1M1) transition[8]. To obtain the Lamb shift we combine our measured $1s2p_{1/2}\ ^3P_0$ lifetime, and the calculated values for the E1M1 decay rate[8], the $1s2p_{1/2}\ ^3P_0$ - $1s2s\ ^3S_1$ E1 matrix element[9], and the $1s2p_{1/2}\ ^3P_0$ - $1s2s\ ^3S_1$ Coulomb splitting[6].

1.3 Production of the $1s2p_{1/2}\ ^3P_0$ state of heliumlike uranium

Few-electron uranium and other very high-Z ions are produced by stripping relativistic ions[10]. Relativistic ions through uranium at energies of up to 1000 MeV/amu are obtained at the Lawrence Berkeley Laboratory's Bevalac[11] The experimentally determined charge state distributions for relativistic uranium ions which have passed through equilibrium thickness targets (typically a few ten's of mg/cm^2 for high-Z targets) is shown in Fig. 3. The processes for electron capture and loss by relativistic heavy ions are well understood and cross sections for ionization, for radiative electron capture and for nonradiative electron capture can be reliably calculated[12,13].

Heliumlike uranium in the $1s2p_{1/2}\ ^3P_0$ state is prepared by capture of an electron in a foil by hydrogenlike uranium The hydrogenlike uranium is made by stripping a beam of 220 MeV/amu uranium 39+ in an equilibrium thickness target. An aluminum target produces an equilibrium charge state distribution of roughly 5% U92+, 30% U91+, 60% U90+, and 5% U89+. The hydrogenlike U91+ fraction is magnetically selected and transported to a 0.9 mg/cm^2 Pd target. In the Pd foil about half of the U91+ ions are converted to heliumlike U90+, with about 1% of these being formed in the $1s2p_{1/2}\ ^3P_0$ state or in states which rapidly decay to the $1s2p_{1/2}\ ^3P_0$ state.

1.4 Measurement of the $1s2p_{1/2}\ ^3P_0$ lifetime

Downstream from the Pd foil we observe, not the 260 eV photon from the $1s2p_{1/2}\ ^3P_0 \rightarrow 1s2s\ ^3S_1$ transition, but instead the 96.01 keV x ray from the subsequent fast decay of the $1s2s\ ^3S_1$ state to the $1s^2\ ^1S_0$ ground state. The 96.01 keV x ray is much easier to detect than the 260 eV photon and the $1s2s\ ^3S_1$ lifetime[7] of 10^{-14} s has no effect on the measured $1s2p_{1/2}\ ^3P_0$ lifetime provided sufficient time is allowed for the initial $1s2s\ ^3S_1$ population to decay.

Fig. 4 shows a spectrum recorded by one of our Ge x-ray detectors collimated to view emission perpendicular to the uranium beam at a point 0.67 cm downstream from the Pd foil. The 96.01 keV x ray from the $1s2p_{1/2}\ ^3P_0$-fed $1s2s\ ^3S_1 \rightarrow 1s^2\ ^1S_0$ decay appears Doppler shifted, as a peak at 77.76 (0.18) keV. We identified this peak by its correct Doppler shift and exponential decay at two different beam energies, 218 MeV/amu and 175 MeV/amu (here determined by the operating conditions of the Bevalac and corrected for energy loss in foils); by the dependence of the Doppler broadened peak width on the angular acceptance of the detector; by the yield[12] using foils of different Z and thickness; by the peaks absence when the foil is removed; and by the lack of any other long-lived low-lying states of heliumlike uranium or hydrogenlike uranium besides the $1s2p_{1/2}\ ^3P_0$ state.

The height of the peak above background was found by a maximum-likelihood fit of a quadratic to the background. The decay curve (Fig. 5), which spans 2.7 decay lengths, is a maximum-likelihood fit of a single exponential to the data. The spectrum shown in Fig. 4 contributes to the first point at 0.67 cm in Fig. 5. The 1/e decay length is 1.182 (0.069) cm, and the 5.8% statistical error dominates our final error in the $1s2p_{1/2}\ ^3P_0$ lifetime. Other contributions to our 6.2% total lifetime error are: 1.2% from the determination of the beam velocity and time dilation using the transverse Doppler shift of the $1s2s\ ^3S_1 \rightarrow 1s^2\ ^1S_0$ transition; and 1.8% from the experimental upper limit to contamination of our signal by cascade feeding. Our value for the $1s2p_{1/2}\ ^3P_0$ lifetime is 54.4 (3.3)ps.

A disadvantage in using the $1s2p_{1/2}\ ^3P_0$-fed $1s2s\ ^3S_1 \rightarrow 1s^2\ ^1S_0$ decay as a signal is to make the measured $1s2p_{1/2}\ ^3P_0$ lifetime sensitive to cascade feeding of the $1s2s\ ^3S_1$ state. States of heliumlike uranium with with principal quantum number (n) < 22 will cascade to the $1s^2\ ^1S_0$ ground state before we begin our measurement of the $1s2p_{1/2}\ ^3P_0$ lifetime. Only the very small population of states with $n \geq 22$ and high total angular momentum (J) can perturb our measurement by cascading down the chain of yrast states (states of J= n) to reach the $1s2p_{3/2}\ ^3P_2$ state. The $1s2p_{3/2}\ ^3P_2$ state (Fig. 2) decays 2/3 of the time to the $1s^2\ ^1S_0$ ground state but also decays 1/3 of the time to the $1s2s\ ^3S_1$ state, contaminating our $1s2s\ ^3S_1 \rightarrow 1s^2\ ^1S_0$ signal. We set a limit to this contamination by searching for the 100.5 keV x ray from the $1s2p_{3/2}\ ^3P_2 \rightarrow 1s^2\ ^1S_0$ transition, which would appear Doppler shifted as an isolated peak at 81.4 keV. The count rate in this supposed peak, after subtraction of the background, is plotted in Fig. 5. The count rate is consistent with zero with an uncertainty which contributes 1.8% to the uncertainty in the $1s2p_{1/2}\ ^3P_0$ decay length. Cascades from high n,J states of hydrogenlike uranium feed only the $2\ ^2P_{3/2} \rightarrow 1\ ^2S_{1/2}$ transition at 102.2 keV.

1.5 Lamb shift in heliumlike uranium

From our $1s2p_{1/2}\ ^3P_0$ lifetime of 54.4 (3.3)ps and Drake's calculated E1M1 decay rate[8] of 0.564(5) $\times$ 10^{10} s^{-1} we obtain a $1s2p_{1/2}\ ^3P_0$ - $1s2s\ ^3S_1$ E1 decay rate of 1.273 (0.113) $\times$ 10^{10} s^{-1}. Using the dipole length formula for the E1 decay rate[9]: $A = 12\alpha k^3 (Z\alpha)^{-2} [0.792+0.759/Z]^2$ (hbar= m= c= 1) we find for k, the $1s2p_{1/2}\ ^3P_0$ - $1s2s\ ^3S_1$ splitting, a value of 260.0 (7.7) eV. Subtracting the calculated Coulomb contribution[6] of 330.4 eV yields a Lamb shift of 70.4 (7.7) eV.

So far we have accounted only for experimental uncertainty; theoretical uncertainty comes from the effect of small terms omitted from the calculations. We estimate that a $Z^{-1} (Z\alpha)^2$ correction to the $1s2p_{1/2}\ ^3P_0$ - $1s2s\ ^3S_1$ E1 matrix element, and a $1/Z$ correction to the E1M1 decay rate, contribute a total of $\approx$ 1 eV to our inferred $1s2p_{1/2}\ ^3P_0$ - $1s2s\ ^3S_1$ splitting; that a $Z^{-2} (Z\alpha)^6$ term contributes $\approx$ 2 eV to the 330.4 eV Coulomb splitting of the $1s2p_{1/2}\ ^3P_0$ - $1s2s\ ^3S_1$ states; and that a $1/Z$ screening correction to the self energy, vacuum polarization and finite nuclear size contributes $\approx$ 1 eV to the Lamb shift. These combine to give a separate theoretical error of 2.4 eV in our extracted value of the Lamb shift.

Our final value[14] for the Lamb shift is then 70.4 (8.1) eV in agreement with the theoretical value[3,4] of 75.3 (0.4) eV.

1.6 Future Lamb shift experiments

With more intense uranium beams and the knowledge gained from these early experiments a direct measurement of the $\approx$ 284 eV $2\ ^2P_{1/2}$ - $2\ ^2S_{1/2}$ splitting[15] in lithiumlike uranium (U^{89+}) to an accuracy of a few-parts in 10^4 appears feasible. When compared with atomic structure calculations of similar accuracy this would test the Lamb shift to 0.1%. The nuclear size of the uranium nucleus is sufficiently well known from muonic atom measurements[16].

2. QED CONTRIBUTIONS TO MAGNETIC MOMENTS OF BOUND ELECTRONS

2.1 Theory

In addition to the QED contribution to the mass of an electron in a Coulomb field (Lamb shift) there is also a QED contribution to the g-factor of the electron in a Coulomb field. This contribution is a bound state effect and is not tested by experiments which measure the g-factor of a free electron. The effect is observable in the hyperfine splitting[17,18] of hydrogenlike atoms and of muonium and in the g-factor[19] of hydrogenlike atoms.

The QED contribution to the electron g-factor in a Coulomb field is tested in the hyperfine structure of hydrogen[18] and the hyperfine structure of muonium[18,20] and in the g-factor of the ground state of hydrogen[21]. Experiments have apparently not been performed for $Z > 1$.

For the hyperfine splitting of hydrogenlike atoms the calculated terms are[17,18],

$$E_F \frac{\alpha}{\pi} \left[C_1(Z\alpha) + C_2(Z\alpha)^2 \ln^2(Z\alpha)^{-2} + C_3(Z\alpha)^2 \ln(Z\alpha)^{-2} + C_4(Z\alpha)^2 + \text{higher order terms} \right] \tag{2}$$

where the higher order terms have not yet been calculated. The contribution to the total hyperfine splitting of the $Z\alpha$ and $(Z\alpha)^2$ terms at different Z computed from Eq. 2 is given in Table I.

The term of order $(Z\alpha)^2$ contributes about 1% of the hyperfine splitting at Z=81 (the anomalous magnetic moment of the free electron contributes roughly 0.1%). In addition, at Z=81, the $(Z\alpha)^2$ term is larger than the lower order $Z\alpha$ term. At very high Z terms of order $(Z\alpha)^3$ and higher could easily be larger than the lower order terms. In the calculation of higher order terms it is necessary to consider the energy of the electron bound by both strong Coulomb and magnetic fields[22].

The g_J factor of a bound electron also has QED contributions which are not present for a free electron and which become relatively large at high Z (Ref. 19). The leading term is $\alpha/\pi\ (Z\alpha)^2$ which contributes 3×10^{-8} in hydrogen and 3×10^{-4} in hydrogenlike uranium. The relative contribution to the g_J factor is smaller and of higher order than for the hyperfine splitting.

2.2 Experiments on hyperfine structure and G_J

Tests of the QED contribution to the hyperfine splitting of an electron bound in a Coulomb field are limited in hydrogen at a few ppm due to the uncertainty in the proton polarizability and in muonium to a few tenths of a ppm due to uncertainties in the muon mass and the fine structure constant[18]. These experiments test the term of order $(Z\alpha)^2$ to about 10% but are probably insensitive to higher order terms. Measurements of the g_J in the ground state of hydrogen[21] achieved a precision of 1×10^{-8} which tests the leading order term to about 30%. Experiments[23] in He^+ are not yet of sufficient sensitivity to see the contribution.

Measurements of the ground state hyperfine structure of hydrogenlike thallium using a storage ring has been suggested by Bemis and Gould[24]. The ground state hydrogenlike thallium ($I = 1/2$) $F=1 \rightarrow F=0$ transition energy is calculated to be 3800 A° without QED corrections and the magnetic dipole decay (M1) rate for $F=1 \rightarrow F=0$ is $\approx 10^3\ s^{-1}$. Confinement of hydrogenlike thallium in a storage ring would then produce a spectrum from the $F=1 \rightarrow F=0$ allowed M1 decay and optical spectroscopy could be used to determine the ground state hyperfine interval.

ACKNOWLEDGMENTS

We thank Mr. Roy Bossingham, Dr. Benedict Feinberg, Mr. Walter L. Kehoe, Dr. Richard McDonald, Professor Richard Mowat, and Dr. Alfred Schlachter for assistance in running the experiment. We thank Dr. Curtis Bemis Jr., Professor Gordon W.F. Drake, Professor Walter R. Johnson, Dr. Peter J. Mohr and Professor Jonathan Sapirstein, for many helpful discussions. We especially thank the operators and the staff and management of the Bevalac for making experiments with few-electron uranium possible. This work was supported by the Director, Office of Energy Research: Office of Basic Energy Sciences, Chemical Sciences Division; and in part by the Office of High Energy and Nuclear Physics, Nuclear Science Division, of the U.S. Department of Energy under Contract No. DE-AC-03-76SF00098.

REFERENCES

1. Erickson, G.W., Phys. Rev. Lett. 27, 780 (1971); Mohr, P.J., Ann. Phys. New York 88, 26 (1974); Mohr, P.J., private communication.
2. For a review of strong field QED, see Brodsky, S.J., and Mohr, P.J., in:

Structure and Collisions of Ions and Atoms. ed. Sellin,I.A., (Springer, Berlin, 1978), Topics in Current Physics, Vol. 5, p. 3.

3. Mohr, P.J., Phys. Rev. Lett. 34, 1050 (1975);
Mohr, P.J., Phys. Rev. A26, 2338 (1982).

4. Johnson, W.R. and Soff, G., Atomic Data and Nucl. Data Tables 33, 405 (1985).

5. Mohr, P.J., in *Relativistic Effects in Atoms, Molecules, and Solids* edited by Malli, G.L. (Plenum, New York, 1983), p. 145.

6. Mohr, P.J., Phys. Rev. A32, 1949 (1985); Mohr, P.J., in *Beam Foil Spectroscopy* edited by Sellin, I.A. and Pegg, D.J., (Plenum, New York, 1976), Vol 1, p. 97; Mohr, P.J., private communication.

7. Lin, C.D., Johnson, W.R., and Dalgarno, A., Phys. Rev. A15, 154 (1977); Parpia, F, and Johnson, W.R., private communication.

8. Drake, G.W.F., Nucl. Instr. Methods in Phys. Research B9, 465 (1985); Drake, G.W.F., private communication.

9. Hillery, M. and Mohr, P.J., Phys. Rev. A 21, 24 (1980); Gould, H., Marrus, R., and Mohr, P.J., Phys. Rev. Lett. 33, 676 (1974).

10. Gould, H., Greiner, D., Lindstrom, P., Symons, T.J.M., and Crawford, H., Phys. Rev. Lett. 52, 180 (1984) (Errata, 52, 1654 [1984]).

11. Alonso, J.R., Avery, R.T., Elioff, T., Force, R.J., Grunder, H.A., Lancaster, H.D., Meneghetti, J.R., Selph, F.B., Stevenson, R.R., and Yord, R.B., Science 217, 1135 (1982).

12. Meyerhof, W.E., Anholt, R., Eichler, J., Gould, H., Munger, Ch., Alonso, J., Thieberger, P., and Wegner, H.E., Phys. Rev. A 32, 3291 (1985); Anholt, R., and Meyerhof, W.E. Phys. Rev A33, 1556 (1986).

13. Anholt, R., Meyerhof, W.E., Gould, H., Munger, Ch., Alonso, J., Thieberger, P., and Wegner, H.E., Phys. Rev. A32, 3302 (1985); Anholt, R., and Gould, H., Relativistic Heavy-Ion-Atom Collisions, to be published in: "Advances in Atomic and Molecular Physics," Bederson, B., ed., Academic Press, Orlando FL (1987); Lawrence Berkeley Laboratory Report No. LBL-20661; Eichler, J., Phys. Rev. A32, 112 (1985); Anholt, R., and Eichler, J., Phys. Rev. A31, 3505 (1985).

14. Munger, C.T., and Gould, H. "Lamb shift in heliumlike uranium (U^{90+})", submitted to Phys. Rev. Lett.

15. Cheng, K.T., Kim, Y. -K., and Desclaux, J.P., Atomic Data and Nucl. Data Tables, 24, 111 (1979); Kim, Y. -K., and Desclaux, J.P., Phys. Rev. Lett. 36, 139 (1976); Armstrong Jr., L., Fielder, W.R., and Lin, D.L. Phys. Rev. A14, 1114 (1976); Fisher, C.F., and Brage, T., private communication.

16. Zumbro, J.D., Shera, E.B., Tanaka, Y., Bemis Jr., C.E., Naumann, R.A., Hoehn, M.V., Reuter, W., and Steffen, R.M., Phys. Rev. Lett. 20, 1888 (1984).

17. Brodsky, S.J., and Erickson, G.W., Phys. Rev. 148, 26 (1966)
18 Sapirstein, J.R., Phys. Rev. Lett. 51, 985 (1983).
19. Grotch, H., Phys. Rev. Lett. 24, 39 (1970); Grotch, H., and Hegstrom, R., Phys. Rev. A4, 59 (1971).
20. Marion, F.G., Beer, W., Bolton, P.R., Egan, P.O., Gardner, C.J., Hughes, V.W., Lu, D.C., Souder, P.A., Orth, H., Vetter, J., Moser, U., zu Putlitz, G., Phys. Rev. Lett. 49, 993 (1982).
21. Tideman and H.G. Robinson, H.G., Phys. Rev. Lett. 39, 602 (1977).
22. Brodsky, S.J., and Primack, J., "The Electromagnetic Interaction of Composite Systems" Ann. Phys. (N.Y.) 52, 315 (1969).
23. Johnson C.E., and Robinson, H.G., Phys. Rev. Lett. 45, 250 (1980).
24. Bemis Jr., C.E., and Gould, H., private communication.

Table I. Bound state QED contributions to hyperfine splitting		
Z	$C_1 (Z\alpha)$	$C_4 (Z\alpha)^2$
1	1×10^{-4}	2×10^{-6}
19	2×10^{-3}	7×10^{-4}
81	8×10^{-3}	1×10^{-2}

Fig. 1. Ratio of the higher order terms in the self-energy to the total self-energy obtained by comparing the series expansion value through term $A_{70}\ (Z\ \alpha)^7$ with a numerical calculation to all orders in $Z\alpha$.

FIG. 2. Energy level diagram of the n=1 and n=2 states of heliumlike uranium. Decay rates, except for the $1s2p_{1/2}\ ^3P_0$ state, are taken from Ref. 7. Energies are taken from Ref. 3,4,7. M1 and M2 decays are magnetic-dipole and magnetic-quadrupole decays respectively and decays without labels are electric-dipole decays. An approximate radiative width is indicated for the $^1P_1$ and $^3P_1$ states.

Fig. 3. Charge state distribution of relativistic uranium after passing through an equilibrium thickness target. A Cu (Z=29) target was used for the 950MeV/amu, 425/amu, and 100 MeV/amu uranium. A Au (Z=79) target was used for the 215 MeV/amu uranium.

FIG. 4. Spectrum recorded by a Ge x-ray detector collimated to view emission perpendicular to the uranium beam at a point 0.67 cm downstream from the Pd foil. This spectrum represents 135 minutes of counting - about 10^8 uranium ions. The Doppler-shifted peak from the decay of $1s2p_{1/2}\ ^3P_0 \rightarrow 1s2s\ ^3S_1 \rightarrow 1s^2\ ^1S_0$ is at 77.8 keV. Cascades from higher excited states would produce a peak at 81.4 keV. Peaks at 72.8 keV and 75.0 keV are Pb $K_{\alpha 2}$ and Pb $K_{\alpha 1}$ x rays, and those at 84.5 keV - 87.3 keV are Pb $K_{\beta 1-\beta 3}$ x rays. Peaks at 56.3 keV and 57.5 keV are Ta $K_{\alpha 2}$ and Ta $K_{\alpha 1}$ x rays, and those at 65.2 and 67.0 keV are are Ta $K_{\beta 1}$ and $K_{\beta 2}$ x rays. Peaks at 45.2 keV - 46.0 keV are Dy $K_{\alpha 2-\alpha 1}$ x rays. Pb and Dy are used for shielding and Ta is used for x-ray detector collimators. The peak at 21.2 keV is scattered Pd $K_{\alpha 1}$ radiation from the Pd foil. Background is caused by bremsstrahlung of the foil electrons in the field of the uranium projectile; by bremsstrahlung of electrons scattered in and ejected from the Pd foil; and by fast nuclear fragments colliding with the Ge in the x-ray detector. Other sources of background may also exist. To reduce background we restricted the scatter of x rays into the detector, held electrons ejected from the foil away from the detector with a magnetic field, and vetoed noise from nuclear fragments using scintillators.

Fig. 5 - Linear plots of the intensity of x rays from the transitions (a) $1s2s\ ^3S_1 \rightarrow 1s^2\ ^1S_0$, and (b) $1s2p_{3/2}\ ^3P_2 \rightarrow 1s^2\ ^1S_0$, as a function of distance downstream from the Pd foil. Each point is the sum of the spectra from two x-ray detectors. The horizontal line in (b) is the fit of a hypothetical constant count rate to the data. The count rate is consistent with zero and sets a limit to the contamination of our signal by cascade feeding.

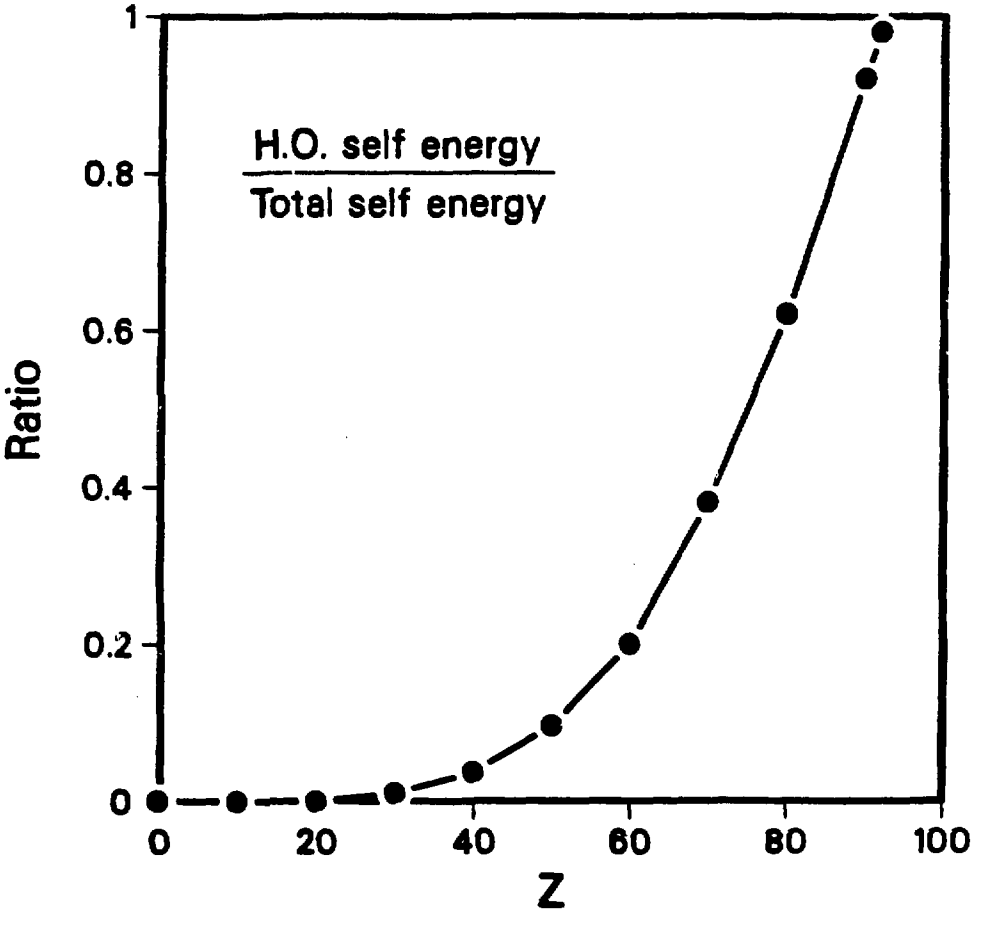
H.O. self energy
Total self energy
Ratio
1
0.8
0.6
0.4
0.2
0
0
20
40
60
80
100
Z
XCG 838-7228

Fig. 1

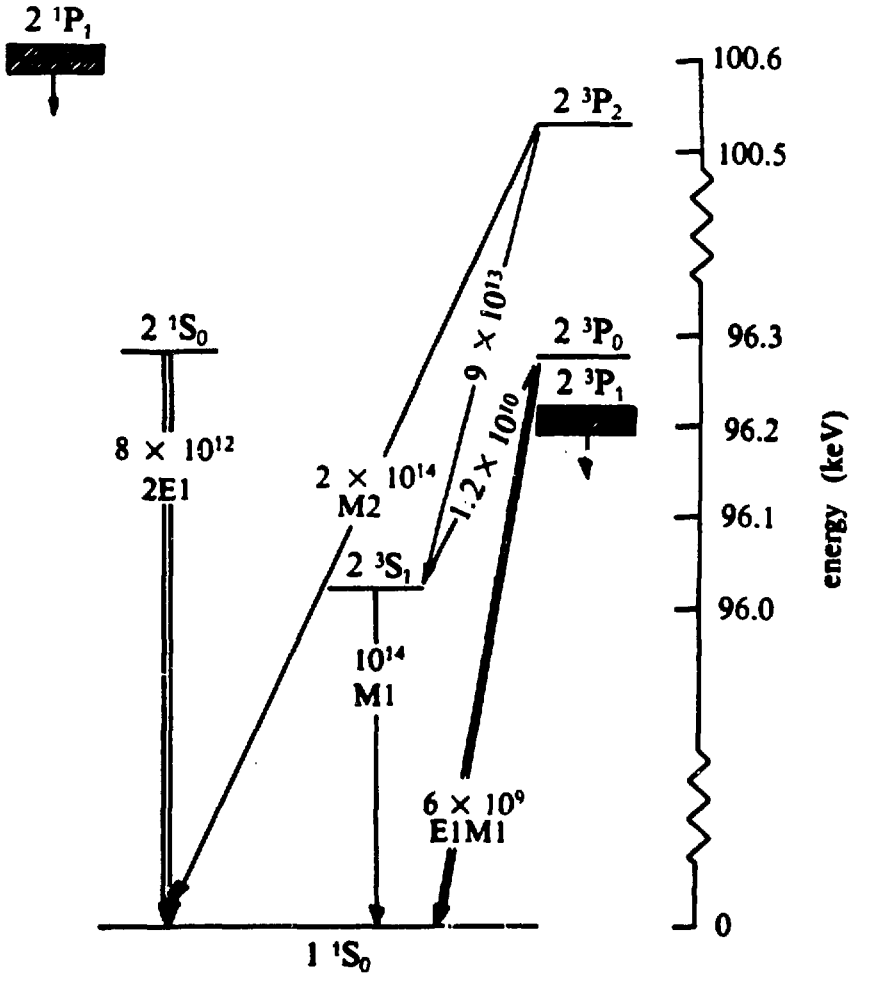
Heliumlike Uranium
2 ¹P₁
2 ³P₂
2 ¹S₀
2 ³P₀
2 ³P₁
2 ³S₁
1 ¹S₀
8 × 10¹²
2E1
2 × 10¹⁴
M2
9 × 10¹³
1.2 × 10¹⁰
10¹⁴
M1
6 × 10⁹
E1M1
100.6
100.5
96.3
96.2
96.1
96.0
0
energy (keV)
XBL 868-2977

Fig. 2

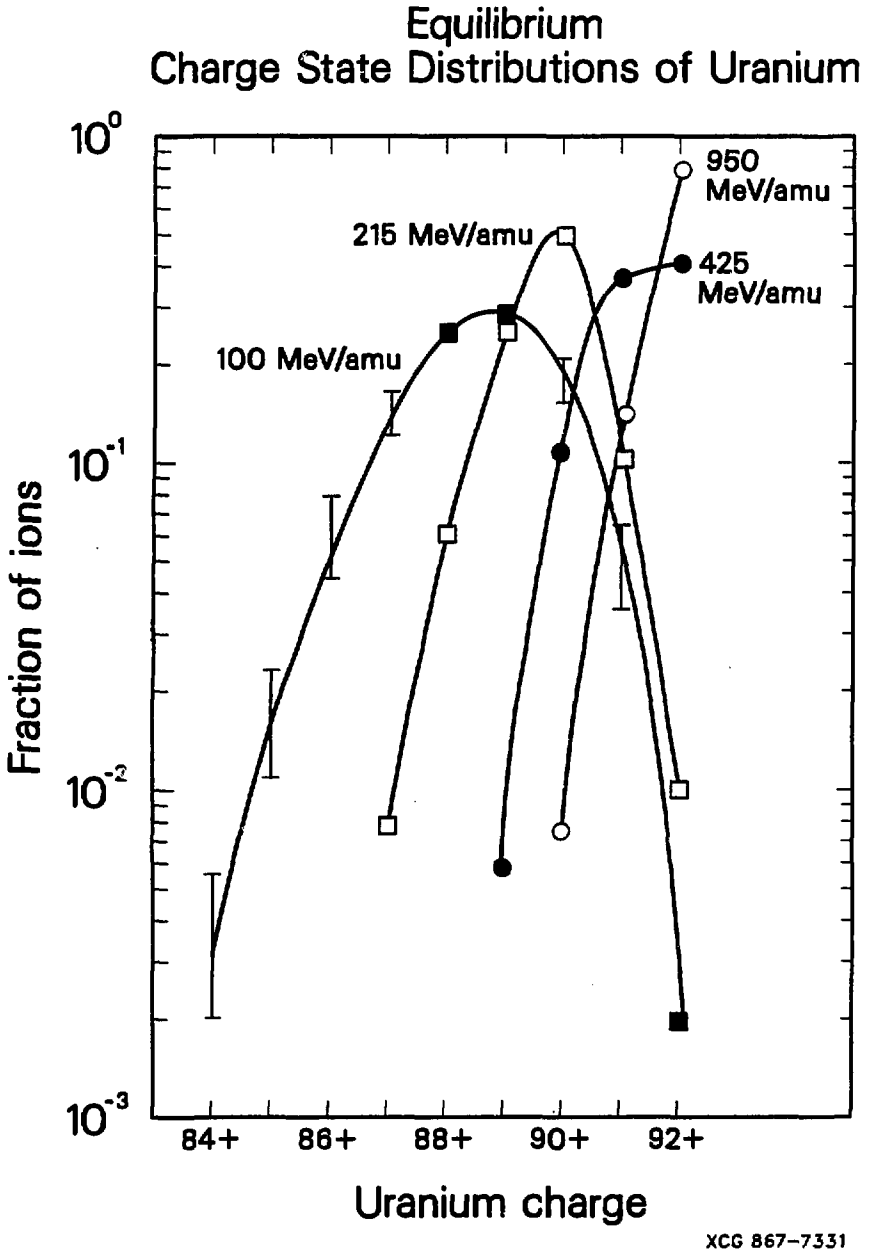
Equilibrium
Charge State Distributions of Uranium
10^0
10^{-1}
10^{-2}
10^{-3}
Fraction of ions
950 MeV/amu
215 MeV/amu
425 MeV/amu
100 MeV/amu
84+
86+
88+
90+
92+
Uranium charge
XCG 867-7331

Fig. 3

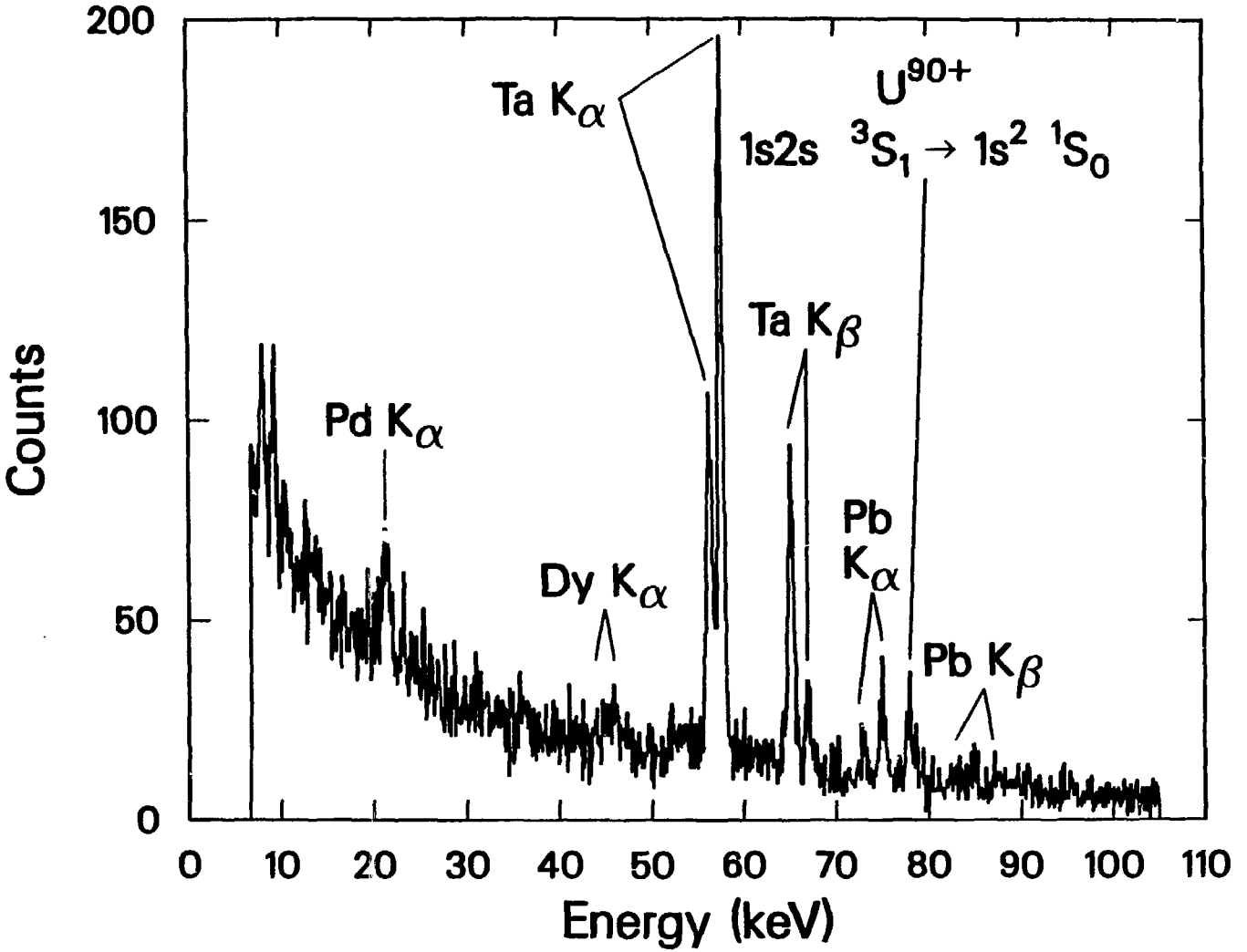

Fig. 4

XCG 867-7332 A

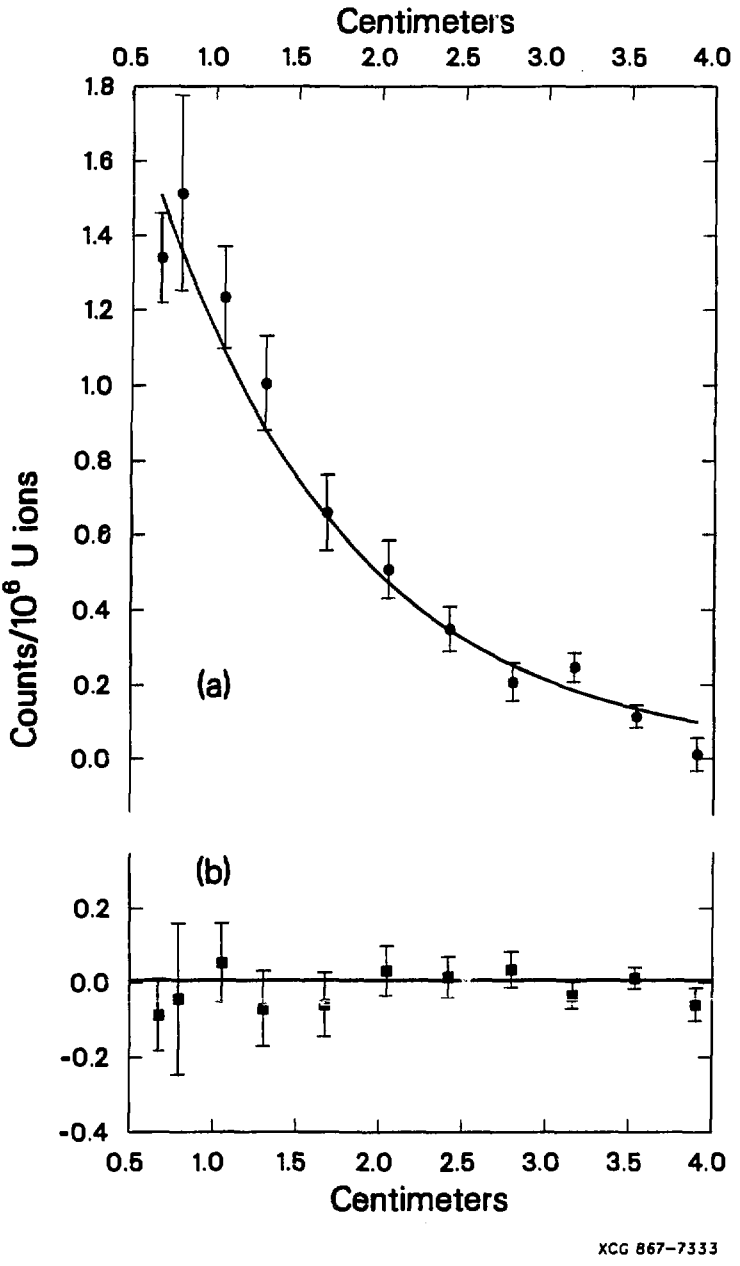
Centimeters
0.5 1.0 1.5 2.0 2.5 3.0 3.5 4.0
1.8
1.6
1.4
1.2
1.0
0.8
0.6
0.4
0.2
0.0
Counts/10^6 U ions
(a)
(b)
0.2
0.0
-0.2
-0.4
0.5 1.0 1.5 2.0 2.5 3.0 3.5 4.0
Centimeters
XCG 867-7333

Fig. 5

This report was done with support from the Department of Energy. Any conclusions or opinions expressed in this report represent solely those of the author(s) and not necessarily those of The Regents of the University of California, the Lawrence Berkeley Laboratory or the Department of Energy.

Reference to a company or product name does not imply approval or recommendation of the product by the University of California or the U.S. Department of Energy to the exclusion of others that may be suitable.